Molecular dynamics study of kinetic boundary condition at an interface between argon vapor and its condensed phase

Tatsuya Ishiyama, Takeru Yano,[a] and Shigeo Fujikawa
Division of Mechanical Science, Graduate School of Engineering, Hokkaido University, Sapporo 060-8628, Japan

(Received 6 November 2003; accepted 29 April 2004; published online 25 June 2004)

The evaporation and condensation at an interface of vapor and its condensed phase is considered. The validity of kinetic boundary condition for the Boltzmann equation, which prescribes the velocity distribution function of molecules outgoing from the interface, is investigated by the numerical method of molecular dynamics for argon. From the simulations of evaporation into vacuum, the spontaneous-evaporation flux determined by the temperature of condensed phase is discovered. Condensation coefficient in equilibrium states can then be determined without any ambiguity. It is found that the condensation coefficient is close to unity below the triple-point temperature and decreases gradually as the temperature rises. The velocity distribution of spontaneously evaporating molecules is found to be nearly a half-Maxwellian at a low temperature. This fact supports the kinetic boundary condition widely used so far. At high temperatures, on the other hand, the velocity distribution deviates from the half-Maxwellian. © *2004 American Institute of Physics.* [DOI: 10.1063/1.1763936]

I. INTRODUCTION

The evaporation from and condensation on a liquid or solid surface have long been an important subject of fundamental researches in physics of fluids. Molecular gas dynamics (rarefied gas dynamics) can give an accurate description of the behavior of vapor adjacent to its condensed (liquid or solid) phase. This has actually been accomplished by solving the Boltzmann equation with a kinetic boundary condition at an interface between vapor and its condensed phase. The boundary condition widely used can be written as[1,2]

$$f^{\mathrm{out}}=\alpha f^{\mathrm{e}}+(1-\alpha)f^{\mathrm{r}} \quad (\xi_z>0), \tag{1}$$

where f^{out} denotes the velocity distribution function of outgoing molecules from the interface and ξ_z is the velocity component normal to the interface. The parameter α $(0<\alpha\leqslant 1)$ has been called the condensation coefficient[3] (the definition of condensation coefficient will be given in Sec. II). f^{e} is a Maxwellian with saturated vapor density ρ_v at the temperature of the condensed phase T_ℓ:

$$f^{\mathrm{e}}=\rho_v \hat{f}^*, \quad \hat{f}^*=\frac{1}{(2\pi RT_\ell)^{3/2}}\exp\left(-\frac{\xi_x^2+\xi_y^2+\xi_z^2}{2RT_\ell}\right), \tag{2}$$

where R is the gas constant and ξ_x and ξ_y are the velocity components tangential to the interface. The symbol $\wedge$ signifies the distribution function normalized by the gas density and the superscript $*$ represents a Maxwellian. For f^{r} in the second term, the diffuse reflection is usually used:

$$f^{\mathrm{r}}=\sigma_w \hat{f}^*, \quad \sigma_w=-\sqrt{\frac{2\pi}{RT_\ell}}\int_{\xi_z<0}\xi_z f^{\mathrm{coll}} d\boldsymbol{\xi}, \tag{3}$$

where f^{coll} is the distribution function of molecules incident on the interface.

A number of problems have been solved on the basis of Eq. (1) (especially in the case of $\alpha=1$, the complete condensation), and thereby various phenomena have been found (see Refs. 1 and 2 and references therein). However, the physical appropriateness of Eq. (1) has never been verified, and the parameter α in Eq. (1) cannot be determined in the framework of the molecular gas dynamics. In the present paper, we shall shed light on the first term αf^{e} in Eq. (1), and examine its validity by the numerical method of molecular dynamics (MD) for argon.

In the following section, we shall clearly state the problem and provide the outline of the analysis. In Sec. III, we describe the method for MD simulations. The numerical results are presented and discussed in Sec. IV. Section V is devoted to conclusions.

II. PROBLEM STATEMENT

Let us consider an interface between a vapor and its condensed phase. The temperature in the bulk condensed phase T_ℓ is assumed to be constant. In order to study the physically appropriate boundary condition, we start from not Eq. (1) but a general expression for f^{out},

$$f^{\mathrm{out}}=f^{\mathrm{sp}}_{\mathrm{evap}}+f^{\mathrm{ref}} \quad (\xi_z>0), \tag{4}$$

where $f^{\mathrm{sp}}_{\mathrm{evap}}$ is a distribution function of molecules spontaneously evaporating from the interface and f^{ref} is defined as $f^{\mathrm{ref}}=f^{\mathrm{out}}-f^{\mathrm{sp}}_{\mathrm{evap}}$. We define the spontaneous evaporation as an evaporation that occurs independently of incident vapor

[a]Author to whom correspondence should be addressed. Telephone: +81-11-706-6430; fax: +81-11-706-7889; electronic mail: yano@mech-me.eng.hokudai.ac.jp

molecules, and therefore, $f^{\mathrm{sp}}_{\mathrm{evap}}$ should be determined by T_ℓ. Equation (4) is general in the sense that an arbitrary f^{out} can be written as the right-hand side of Eq. (4). The essential points are whether $f^{\mathrm{sp}}_{\mathrm{evap}}$ exists and how $f^{\mathrm{sp}}_{\mathrm{evap}}$ is given if it exists.

Since we start from Eq. (4), in the equilibrium state of T_ℓ, f^{out} is equal to $f^{\mathrm{e}}(\xi_z>0)$, and hence $f^{\mathrm{ref}}=f^{\mathrm{e}}-f^{\mathrm{sp}}_{\mathrm{evap}}$. Since $f^{\mathrm{sp}}_{\mathrm{evap}}$ is independent of vapor, all the effects of incident vapor molecules are included in f^{ref}. Therefore, f^{ref} may be regarded as the distribution function of reflected molecules.

Equation (4) enables us to validate the first term in Eq. (1) by examining $f^{\mathrm{sp}}_{\mathrm{evap}}$. In an extreme situation of no incident molecules, we immediately have

$$f^{\mathrm{out}}=f^{\mathrm{sp}}_{\mathrm{evap}}, \quad f^{\mathrm{ref}}=0. \tag{5}$$

In Sec. IV, we shall realize such a situation in an MD simulation of evaporation into vacuum, and determine $f^{\mathrm{sp}}_{\mathrm{evap}}$ as a distribution function of molecules evaporating into vacuum. The existence of the spontaneous evaporation is thus confirmed, and this means that our starting point (4) is valid. It will be shown that $f^{\mathrm{sp}}_{\mathrm{evap}}$ is a half-Maxwellian in relatively low temperature cases and is equal to $\alpha f^{\mathrm{e}}(\xi_z>0)$ with α defined below. The result supports the physical validity of the first term in Eq. (1).

Although several authors[4–9] have executed MD studies for evaporation and condensation at the interface, the spontaneous evaporation has never been examined. On the contrary, they have tried to count the number of reflected molecules in equilibrium states.[4–9] However, it seems to be intrinsically difficult[10] because molecules experience complicated interactions at the interface; the spontaneous evaporation can be determined only in the vacuum evaporation MD simulation as will be done in the present paper.

Next, we shall explain the relation between the condensation coefficient and the parameter α. From Eq. (4), it can be readily seen that the molecular mass fluxes of f^{out}, $f^{\mathrm{sp}}_{\mathrm{evap}}$, and f^{ref} satisfy a relation,

$$\langle J_{\mathrm{ref}}\rangle=\langle J_{\mathrm{out}}\rangle-\langle J^{\mathrm{sp}}_{\mathrm{evap}}\rangle, \tag{6}$$

where $\langle J_{\mathrm{ref}}\rangle=\int_{\xi_z>0}\xi_z f^{\mathrm{ref}}d\boldsymbol{\xi}$, $\langle J_{\mathrm{out}}\rangle=\int_{\xi_z>0}\xi_z f^{\mathrm{out}}d\boldsymbol{\xi}$, and $\langle J^{\mathrm{sp}}_{\mathrm{evap}}\rangle=\int_{\xi_z>0}\xi_z f^{\mathrm{sp}}_{\mathrm{evap}}d\boldsymbol{\xi}$. Note that the evaporation flux $\langle J^{\mathrm{sp}}_{\mathrm{evap}}\rangle$ is a function of only T_ℓ under the present assumptions. Application of the mass conservation law at the interface leads to the definition of the condensed mass flux $\langle J_{\mathrm{cnds}}\rangle$,

$$\langle J_{\mathrm{cnds}}\rangle=\langle J_{\mathrm{coll}}\rangle-\langle J_{\mathrm{ref}}\rangle, \tag{7}$$

where $\langle J_{\mathrm{coll}}\rangle=-\int_{\xi_z<0}\xi_z f^{\mathrm{coll}}d\boldsymbol{\xi}$ (see Fig. 1). The definitions of condensation coefficient α_c and evaporation coefficient α_e can then be given as

$$\alpha_c=\frac{\langle J_{\mathrm{cnds}}\rangle}{\langle J_{\mathrm{coll}}\rangle}, \quad \alpha_e=\frac{\langle J^{\mathrm{sp}}_{\mathrm{evap}}\rangle}{\langle J_{\mathrm{out}}\rangle_{\mathrm{e}}}, \tag{8}$$

where $\langle J_{\mathrm{out}}\rangle_e=\rho_v\sqrt{RT_\ell/(2\pi)}$ is the outgoing mass flux at the equilibrium state. While α_e is determined only by T_ℓ, α_c in general depends on the both vapor and condensed phase.

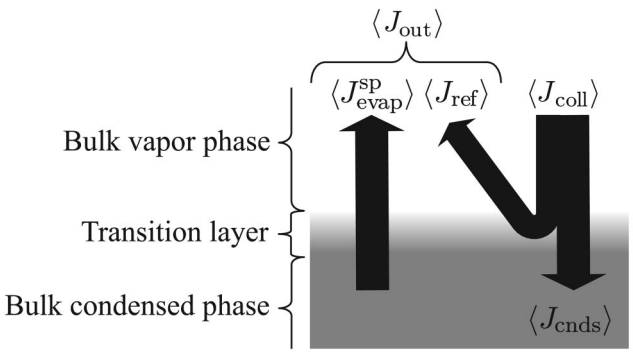

FIG. 1. Molecular fluxes at the interface.

In the equilibrium state, since $\langle J_{\mathrm{out}}\rangle=\langle J_{\mathrm{coll}}\rangle$, we have $\langle J_{\mathrm{cnds}}\rangle=\langle J^{\mathrm{sp}}_{\mathrm{evap}}\rangle$ from Eqs. (6) and (7), and hence $\alpha_c=\alpha_e$. In this paper, we define α as

$$\alpha=\frac{\langle J^{\mathrm{sp}}_{\mathrm{evap}}\rangle}{\langle J_{\mathrm{out}}\rangle_e}, \tag{9}$$

which is equal to α_e and α_c in the equilibrium state. We shall evaluate α for a wide temperature range including the triple point.

III. COMPUTATIONAL METHOD

We consider the dynamics of molecules at an interface between vapor and condensed phases of argon. The phenomenon concerned is assumed as one dimensional in a macroscopic sense, i.e., the interface is assumed as planar in a macroscopic sense and normal to the z axis (see Fig. 2).

A. Equilibrium simulation

To begin with, we describe the method for equilibrium MD simulations for argon. The computational method is almost the same as those developed in Refs. 4, 11, 12, where a system of N molecules is considered in a simulation cell with dimensions $L_x\times L_y\times L_z$ for a specified average temperature T_ℓ. The simulations are executed for $T_\ell=70$, 75, 80, 85, 90, 100, 110, 120, and 130 K. A vapor-liquid equilibrium is obtained between the triple-point temperature (83.8 K) and the critical-point temperature (150.7 K), and a vapor-solid equilibrium is obtained below the triple-point temperature, where the sublimation occurs.

As an intermolecular potential of argon molecules for $85\,\mathrm{K}\leqslant T_\ell\leqslant 130\,\mathrm{K}$, we use a 12-6 type Lennard-Jones potential[13]

$$\phi(r)=4\epsilon\left[\left(\frac{\sigma}{r}\right)^{12}-\left(\frac{\sigma}{r}\right)^{6}\right], \tag{10}$$

where the particle diameter σ is 3.405 Å and the potential depth ϵ/k is 119.8 K (k is the Boltzmann constant). The Lennard-Jones potential however gives poor saturated vapor density below the triple point. To obtain reliable results for $T_\ell=70$, 75, and 80 K, we use the Dymond–Alder potential,[14] which is a numerically tabulated one. The

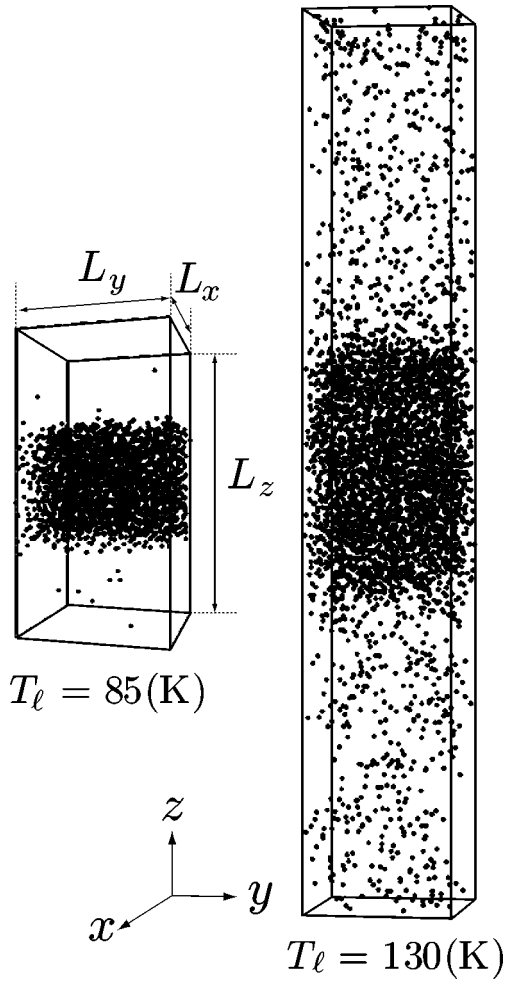

FIG. 2. Snapshots of equilibrium simulations in relatively low and high temperature cases.

Dymond–Alder potential gives excellent results for the heat of sublimation and atomic separation of solid argon[15] and the saturated vapor density (Fig. 3).

The other parameters are as follows: In the cases of $70\,\mathrm{K} \leqslant T_\ell \leqslant 100\,\mathrm{K}$, the cell length $L_z = 100$ Å and the total number of molecules $N = 2000$, while in higher temperature cases of $110\,\mathrm{K} \leqslant T_\ell \leqslant 130\,\mathrm{K}$, we increase L_z to 300 Å and N to 4000. The surface area $L_x \times L_y$ is fixed to 50×50 Å^2 in all cases.

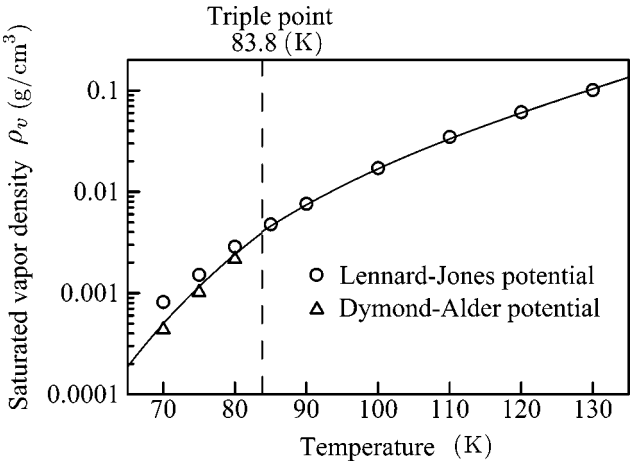

FIG. 3. Saturated vapor density calculated with the Lennard-Jones potential and the Dymond–Alder potential. The solid line is a new equation of state for argon proposed by Tegeler *et al.* (Ref. 16).

Newton's equations of motion for N molecules in the cell are solved by the leap-frog method with the time step 1 fs. For the both potentials, the cutoff radius is set to 15 Å. The periodic boundary conditions are imposed for all three directions of the simulation cell.

When a steady state is attained, a thick condensed phase is formed at about the center of the cell as shown in Fig. 2. The thickness of the bulk condensed phase is at least 30 Å in low temperature cases and 60 Å or more in high temperature cases. After that, the simulation is continued until 10 ns and the configuration of molecules is sampled every 400 fs. This yields 25 000 samples. Since there are two interfaces in the cell, we have 50 000 samples in one simulation. The ensemble averages are evaluated from $N_s = 50\,000$ sampled configurations.

In MD simulations, an averaged density can be calculated as

$$\rho = \frac{1}{N_s \Xi_p} \sum_{N_s} \sum_{i \in \Xi_p} m^i, \tag{11}$$

where Ξ_p is a volume element in the physical space, m^i is the mass of the ith molecule ($m^i = m$, m is the mass of a molecule). The summation $\Sigma_{i \in \Xi_p} m^i$ means the mass of the molecules inside Ξ_p. One can also calculate a flux J by counting the number of molecules passing through a unit area per unit time, and then the ensemble-averaged flux is calculated as $\langle J \rangle = (1/N_s)\Sigma_{N_s} J$. The averaged bulk vapor density (saturated vapor density) ρ_v, bulk liquid (or solid) density ρ_ℓ, and $\langle J_{\mathrm{coll}} \rangle_e$ and $\langle J_{\mathrm{out}} \rangle_e$ obtained from the equilibrium simulations are shown in Table I, where $\langle J_{\mathrm{coll}} \rangle_e$ is the mass flux of molecules incident on the interface in the equilibrium state. The numerical results show good agreement with corresponding experimental ones. Clearly, an equilibrium condition $\langle J_{\mathrm{out}} \rangle_e = \langle J_{\mathrm{coll}} \rangle_e$ is satisfied.

The averaged density profiles are shown in Fig. 4. Note that, here and hereafter, one of the two interfaces in a cell, facing in the positive z direction, is presented and discussed. The density in the transition layer can be well fitted with a function,

$$\rho(z) = \frac{\rho_v + \rho_\ell}{2} + \frac{\rho_v - \rho_\ell}{2} \tanh\left(\frac{z - Z_m}{0.455\delta} \right), \tag{12}$$

where Z_m denotes the center of the transition layer and δ the 10–90 thickness (see Table I). Z_m and δ are obtained by a nonlinear least-squares method (Levenberg–Marquardt method[17]). These values are affected by the simulation cell size and temperature. We introduce the following coordinate:

$$z^* = \frac{z - Z_m}{\delta}, \tag{13}$$

and thus we can compare various physical quantities of different temperatures in the z^* coordinate. As shown in Fig. 4, the bulk vapor phase is well developed in $z^* \gtrsim 2$ for all cases of T_ℓ.

TABLE I. The results of equilibrium simulations. The values in parentheses in ρ_v and ρ_ℓ columns are experimental ones (Ref. 16).

T_ℓ (K)	ρ_v (10^{-3} g/cm^3)	ρ_ℓ (g/cm^3)	δ (Å)	$\langle J_{\rm coll}\rangle_e$ [g/(cm^2 s)]	$\langle J_{\rm out}\rangle_e$ [g/(cm^2 s)]
70	0.44(0.50)	1.55 (—)	4.60	2.18	2.19
75	1.02(1.16)	1.53 (—)	4.96	5.38	5.36
80	2.16(2.41)	1.50 (—)	5.32	11.13	11.14
85	4.77(4.59)	1.38 (1.41)	6.27	25.15	25.16
90	7.61(7.44)	1.35 (1.38)	7.09	40.64	40.66
100	17.13(16.87)	1.30 (1.31)	8.35	97.56	97.53
110	34.86(33.30)	1.23 (1.24)	10.75	204.09	203.38
120	61.15(60.16)	1.15 (1.16)	12.31	372.28	372.26
130	101.28(103.61)	1.06 (1.07)	15.71	637.66	637.47

B. Vacuum simulation

We now turn to the simulation method for evaporation into vacuum. As an initial condition for the vacuum simulation, a configuration at an arbitrary time in the vapor–liquid or vapor–solid equilibrium state of T_ℓ is used, for which Z_m and δ are known. The periodic boundary conditions are applied in the x and y directions alone. The top and bottom of the cell are assumed to be open to the vacuum. Molecules can evaporate into vacuum but cannot come from vacuum. The number of molecules in the cell are therefore gradually reduced as time goes on. As a result, the thickness of the condensed phase decreases with time, and the transition layer moves in the negative z direction, accordingly. Then, another coordinate transformation may be useful,

$$z^* = \frac{z-(Z_m - v_s t)}{\delta}, \quad v_s = \frac{J_s}{\rho_\ell}, \tag{14}$$

where t is the time from the beginning of the vacuum simulation, J_s is a nonaveraged molecular flux evaporating into vacuum, and v_s is the speed of the moving coordinate. Here, we use the same symbol z^* as in Eq. (13), but this would not lead to confusion. At each time step, we estimate the evaporation flux J_s at $z^* = L_g^*$, and eliminate the molecules in a region $z^* > L_g^*$, a virtual vacuum (see Fig. 5).

Using the velocity scaling method,[18] we control the temperature of the condensed phase in the region $z^* < -L_c^*$ as shown schematically in Fig. 5. The size of L_c^* is chosen so that the averaged temperature in the bulk condensed phase can be fixed to a specified T_ℓ; we found that $L_c^* = 0$, 0.5, and 1 give good results. Since z^* is the moving coordinate, the molecules to which the velocity scaling is applied change with time. The temperature control technique is essential to realize a steady state. If an inadequate temperature control is applied, a steady state may not be realized or the reference temperature may not be determined uniquely.[19] Our temperature control works well. In fact, the averaged temperature and density in the bulk condensed phase are almost uniform and equal to T_ℓ and ρ_ℓ, respectively.

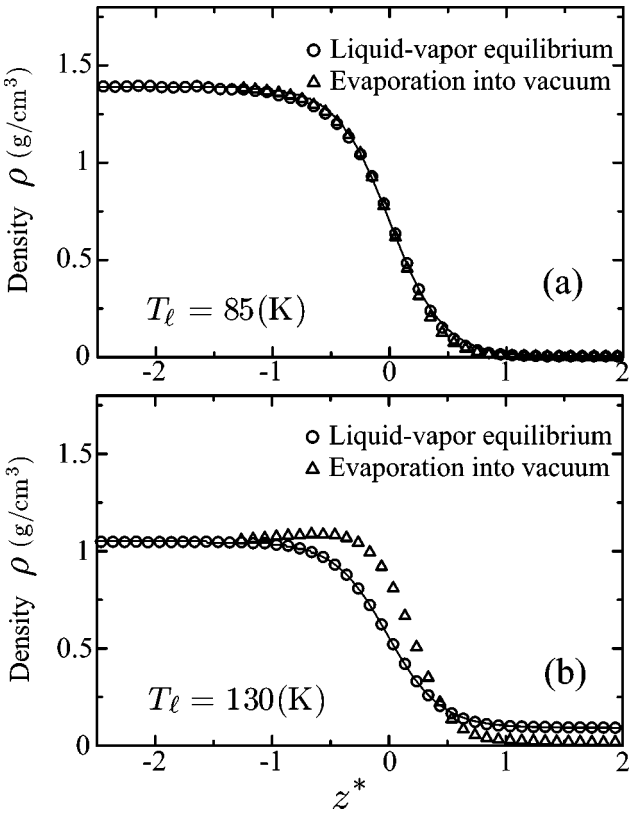

FIG. 4. Density profiles around the interface in equilibrium simulations and vacuum simulations. The solid line represents Eq. (12) ($\Xi_p = L_x L_y \Delta z^*$, $\Delta z^* = 0.1$). (a) $T_\ell = 85$ K, (b) $T_\ell = 130$ K.

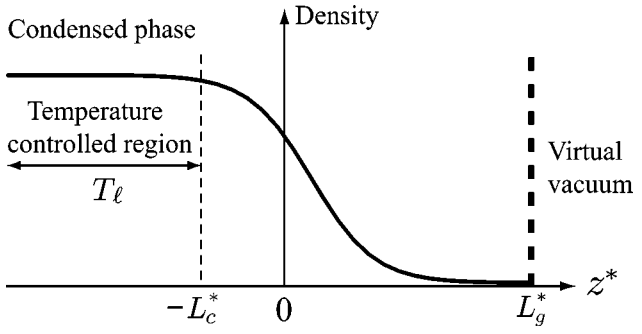

FIG. 5. Schematic of simulation of evaporation into the virtual vacuum on the moving coordinate z^* defined by Eq. (14).

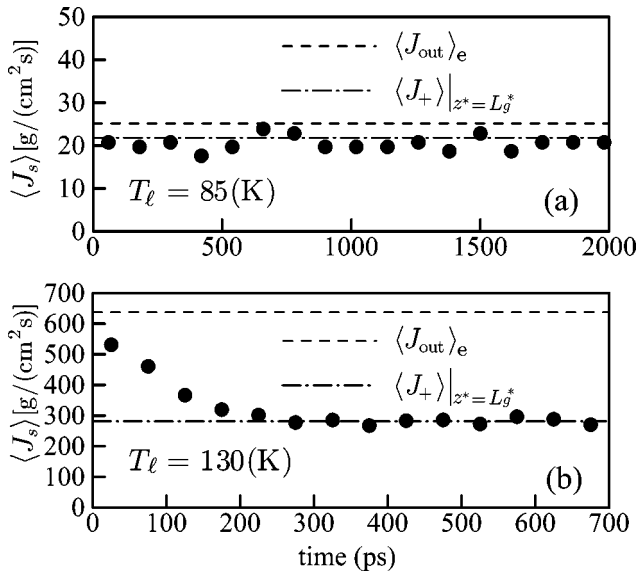

FIG. 6. $\langle J_s\rangle$ in vacuum simulations. (a) $T_\ell = 85$ K, (b) $T_\ell = 130$ K. In this figure, $\langle J_-\rangle$ is zero ($L_g^*=4.0$, $L_c^*=1.0$). Note that $\langle J_s\rangle$ is defined at $z^* = L_g^*$.

At the time when the number of molecules in a region $z^* < L_g$ decreases to 1000 due to the evaporation into vacuum, we stop the simulation in order to avoid sampling erroneous configurations. This sometimes leads to the shortage of the number of samples for ensemble averages. To compensate this, we execute seven more simulations starting from different initial conditions.

IV. RESULTS AND DISCUSSION

A. Spontaneous-evaporation flux and condensation coefficient in equilibrium state

The temporal evolution of molecular flux $\langle J_s\rangle$ in the vacuum simulation is plotted for $T_\ell = 85$ and 130 K in Fig. 6. For the both temperatures, one can see that after an initial transient state, an almost steady state is realized and $\langle J_s\rangle$ can be regarded as constant except for small fluctuation. In Figs. 6 and 7, $\langle J_{+(-)}\rangle$ denotes an averaged flux in the positive (negative) z^* direction after the steady state is established.

In the steady evaporation state, the averaged fluxes are calculated at various points on the moving coordinate. Figure 7 shows the spatial distributions of outgoing flux $\langle J_+\rangle$ and

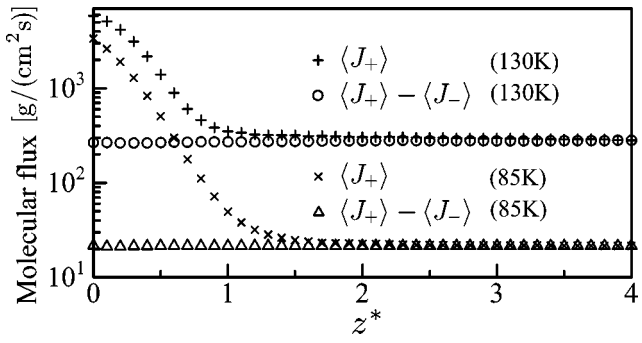

FIG. 7. The spatial distribution of fluxes in the steady evaporation state in vacuum simulations ($T_\ell = 85$ and 130 K, $L_g^*=4.0$, $L_c^*=1.0$).

TABLE II. The results of vacuum simulations.

T_ℓ (K)	$\langle J_{\rm evap}^{\rm sp}\rangle$ [g/(cm^2 s)]	α	ρ_c (10^{-3} g/cm^3)	$\alpha\rho_v/2$ (10^{-3} g/cm^3)
70	2.16	0.985	0.26	0.21
75	5.16	0.963	0.48	0.49
80	10.10	0.906	0.91	0.98
85	21.83	0.868	2.06	2.07
90	33.96	0.835	3.08	3.18
100	74.61	0.765	6.54	6.55
110	137.74	0.678	11.78	11.82
120	213.27	0.573	17.23	17.52
130	281.80	0.442	22.21	22.39

the net flux $\langle J_+\rangle - \langle J_-\rangle$. Clearly, the spatial uniformity of the net flux in Fig. 7 indicates the steady state. $\langle J_+\rangle$ agrees with the net flux for $z^* \gtrsim 2$, because no molecules come from the virtual vacuum $z^* > L_g^* = 4$. From the results of vacuum simulations for different L_g^*'s ($L_g^* = 2$, 3, and 4), we confirm that the net flux is hardly affected by the size of L_g^* and determined only by T_ℓ. That is, the spontaneous-evaporation flux $\langle J_{\rm evap}^{\rm sp}\rangle$ certainly exists and can be defined by the net flux in the vacuum simulation:

$$\langle J_{\rm evap}^{\rm sp}\rangle = \langle J_+\rangle - \langle J_-\rangle = \langle J_+\rangle|_{z^*=L_g^*}. \tag{15}$$

The spontaneous-evaporation fluxes $\langle J_{\rm evap}^{\rm sp}\rangle$ obtained in the vacuum simulation are presented in Table II.

As shown in Fig. 6(a), the difference between $\langle J_{\rm out}\rangle_e$ (broken line) and $\langle J_+\rangle|_{z^*=L_g^*} = \langle J_{\rm evap}^{\rm sp}\rangle$ (dash-dotted line) is small for $T_\ell = 85$ K. This implies that $\langle J_{\rm ref}\rangle$ determined from Eq. (6) is small in the equilibrium state at low temperature. In the case of $T_\ell = 130$ K shown in Fig. 6(b), $\langle J_{\rm out}\rangle_e$ in the equilibrium state is considerably large compared with $\langle J_+\rangle|_{z^*=L_g^*} = \langle J_{\rm evap}^{\rm sp}\rangle$. That is, $\langle J_{\rm ref}\rangle$ amounts to half or more of $\langle J_{\rm out}\rangle_e$ in the equilibrium state at $T_\ell = 130$ K.

Once the flux $\langle J_{\rm evap}^{\rm sp}\rangle$ is obtained, the condensation coefficient in the equilibrium state α can be easily evaluated from its definition, Eq. (9). In Fig. 8 (see also Table II), we plot α for argon as a function of T_ℓ. The results of previous MD simulations[19–21] are also shown for comparison. As men-

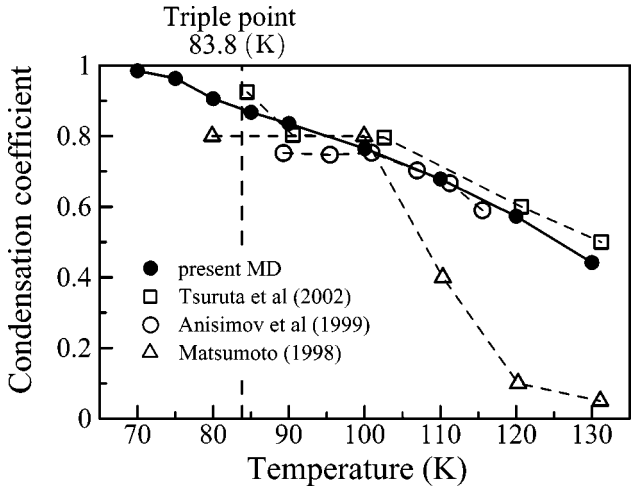

FIG. 8. Condensation coefficient α for argon at equilibrium conditions.

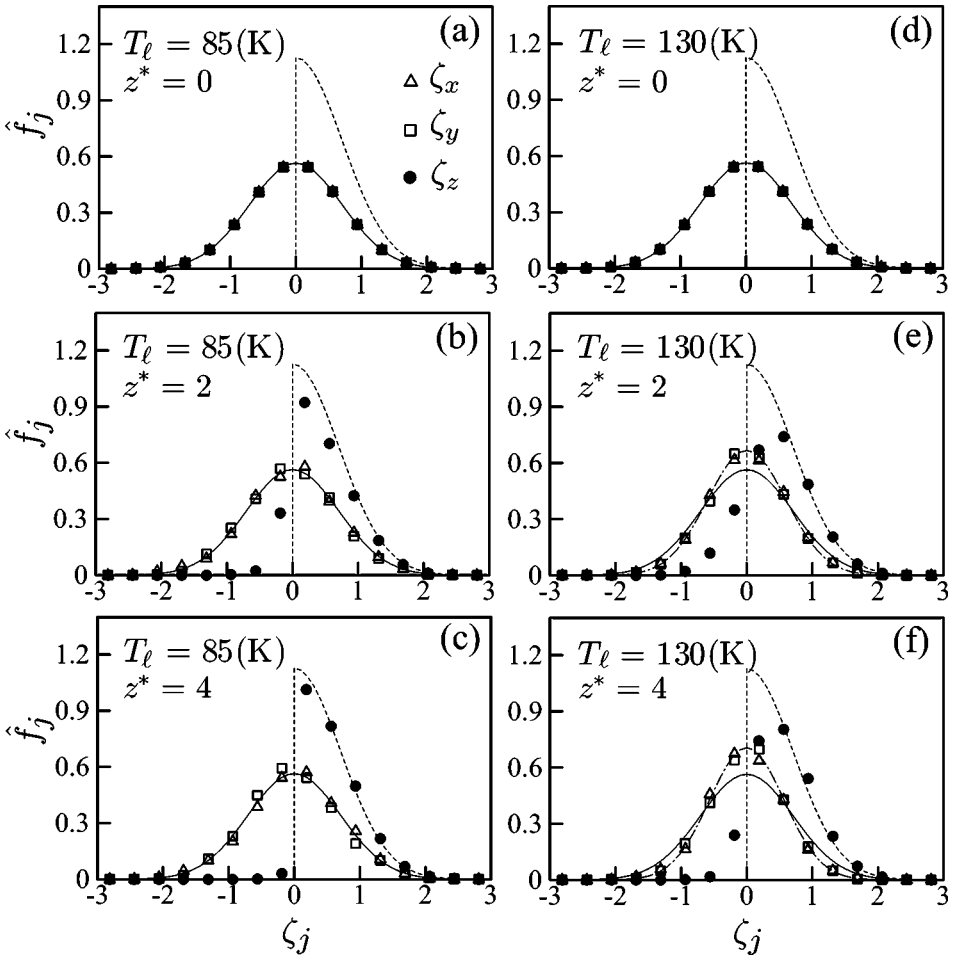

FIG. 9. Velocity distribution of molecules evaporating into vacuum in the case of $L_g^*=4$. (a) $T_\ell=85$ K and $z^*=0$, (b) $T_\ell=85$ K and $z^*=2$, (c) $T_\ell=85$ K and $z^*=4$, (d) $T_\ell=130$ K and $z^*=0$, (e) $T_\ell=130$ K and $z^*=2$, (f) $T_\ell=130$ K and $z^*=4$. The solid curve indicates a one-dimensional normalized Maxwellian $(1/\sqrt{\pi})\exp(-\zeta_j^2)$ and the dashed curve a one-dimensional normalized half-Maxwellian $(2/\sqrt{\pi})\exp(-\zeta_j^2)$ $(\zeta_j>0)$. The dash-dotted curves are a Maxwellian with temperatures evaluated by MD simulation, $\sqrt{T_\ell/(T_2\pi)}\exp(-\zeta_i^2 T_\ell/T_2)$ with $T_2=92.5$ K at $z^*=2$ and $T_2=84.1$ K at $z^*=4$ ($\Xi_p=L_xL_y\Delta z^*$, $\Delta z^*=0.2$, $\Xi_v^j=\Delta\zeta$, $\Delta\zeta=0.375$).

tioned in Sec. II, the previous authors counted reflected molecules in equilibrium states and evaluated $\langle J_{\mathrm{cnds}}\rangle$ by using Eq. (7). Although some ambiguity is inevitably involved in such a treatment,[10] the discrepancy of their results from ours is small except for the result in Ref. 21. It can be seen that α approaches unity below the triple point and monotonically decreases as the temperature rises.

The temperature dependence of α is qualitatively similar to those reported in several experimental studies for various materials other than argon (Thran *et al.*,[22] Kossacki *et al.*[23]). For example, Fujikawa *et al.*[24] have conducted experimental studies on the condensation coefficient of methanol by combining a shock-tube experiment with an asymptotic analysis[2] based on the kinetic theory. They have shown that α is strongly affected by temperature and density conditions. The long history on the determination of the condensation coefficient can be found in Cammenga's monograph.[25]

B. Velocity distribution of spontaneous evaporation

We shall evaluate the velocity distribution of molecules evaporating into vacuum $f_{\mathrm{evap}}^{\mathrm{sp}}$. In MD simulations, a velocity distribution function f can be calculated as

$$f=\rho\hat{f}_x\hat{f}_y\hat{f}_z, \quad \hat{f}_j=\frac{1}{\rho N_s \Xi_p \Xi_v^j}\sum_{N_s}\sum_{i\in(\Xi_p\cap\Xi_v^j)} m^i, \qquad (16)$$

where $\hat{f}_j$ is the marginal distribution of the j component of molecular velocity $(j=x,y,z)$, Ξ_v^j a one-dimensional volume element in the j direction in the molecular velocity space, and $\Xi_p\cap\Xi_v^j$ four-dimensional one in the six-dimensional phase space.[26] Note that ξ_x, ξ_y, and ξ_z are assumed to be independent random variables.[27] In all cases, $\hat{f}_x$ and $\hat{f}_y$ are equal due to the isotropy in the (x,y) plane. The distributions of molecules evaporating into the vacuum at $z^*=0$, 2, and 4 are plotted for $T_\ell=85$ K and 130 K in Fig. 9. The abscissa $\zeta_j=\xi_j/\sqrt{2RT_\ell}$ is the j component of normalized molecular velocity.

As shown in Figs. 9(a) and 9(d), at $z^*=0$ (center of the transition layer), all of $\hat{f}_j$'s agree with a solid curve, a one-dimensional normalized Maxwellian $(1/\sqrt{\pi})\exp(-\zeta_j^2)$.[28] This means that molecules are in a local equilibrium state around $z^*=0$. When $T_\ell=85$ K, at $z^*=2$, $\hat{f}_z$ is distorted from Maxwellian [see Fig. 9(b)] and it develops into a one-dimensional normalized half-Maxwellian $(2/\sqrt{\pi})\times\exp(-\zeta_j^2)$ $(\zeta_j>0)$ at $z^*=4$ [Fig. 9(c)]. That is, in the three-dimensional form,

$$\hat{f}_{\mathrm{evap}}^{\mathrm{sp}}=2\hat{f}^* \quad (\xi_z>0), \qquad (17)$$

where $\hat{f}^*$ is the normalized Maxwellian defined in Eq. (2), $\hat{f}_{\mathrm{evap}}^{\mathrm{sp}}=f_{\mathrm{evap}}^{\mathrm{sp}}/\rho_c$, and ρ_c is the vapor density evaporating into vacuum. On the other hand, when $T_\ell=130$ K, both $\hat{f}_x$ and $\hat{f}_y$

become Maxwellian with lower temperatures [see Figs. 9(e) and 9(f)], and $\hat{f}_z$ deviates from the half-Maxwellian at $z^*=4$ [see Fig. 9(f)]. Zhakhovskii and Anisimov[29] also examined the distribution function $\hat{f}_z$ for evaporation into vacuum, and obtained the results similar to those in the present paper. Our results make $\hat{f}^{\rm sp}_{\rm evap}$ more clear than their ones.

The vapor density evaporating into vacuum ρ_c can be evaluated from Eq. (11). The result is shown in Table II.

C. Kinetic theory analysis for half-Maxwellian

In the preceding section, by using MD simulations, we have shown that $f^{\rm sp}_{\rm evap}$ is the half-Maxwellian in a low temperature case [Eq. (17)]. In this section, we shall analyze the behavior of the vapor evaporating into vacuum by using the kinetic theory of gases.

First, we shall analytically prove that $f^{\rm sp}_{\rm evap}=\alpha f^{\rm e}(\xi_z>0)$ if $\hat{f}^{\rm sp}_{\rm evap}(=f^{\rm sp}_{\rm evap}/\rho_c)$ is the half-Maxwellian with T_ℓ. Suppose that $\hat{f}^{\rm sp}_{\rm evap}$ is the half-Maxwellian (17). Then,

$$\langle J^{\rm sp}_{\rm evap}\rangle=\int \xi_z f^{\rm sp}_{\rm evap}d\boldsymbol{\xi}=\rho_c\sqrt{\frac{2RT_\ell}{\pi}}. \tag{18}$$

On the other hand, from the definition of α, Eq. (9),

$$\langle J^{\rm sp}_{\rm evap}\rangle=\alpha\langle J_{\rm out}\rangle_e=\alpha\rho_v\sqrt{\frac{RT_\ell}{2\pi}}. \tag{19}$$

Elimination of $\langle J^{\rm sp}_{\rm evap}\rangle$ from Eqs. (18) and (19) immediately gives

$$\rho_c=\alpha\frac{\rho_v}{2}. \tag{20}$$

We therefore obtain

$$f^{\rm sp}_{\rm evap}=\alpha\rho_v\hat{f}^*=\alpha f^{\rm e}\quad(\xi_z>0) \tag{21}$$

[see Eq. (2)]. Thus, the first term in Eq. (1) is validated physically.

In the above proof, Eq. (20) is a consequence deduced from the assumption that $\hat{f}^{\rm sp}_{\rm evap}$ is the half-Maxwellian. However, the numerical result shows that Eq. (20) holds even in high temperature cases, where $\hat{f}^{\rm sp}_{\rm evap}$ is not the half-Maxwellian [see Table II and Fig. 9(f)]. This may be explained as follows: although $\hat{f}^{\rm sp}_{\rm evap}$ in the case of $T_\ell=130$ K is distorted from the half-Maxwellian, the difference is limited for small $|\boldsymbol{\xi}|$, and therefore the difference in the mass fluxes is small [see Eq. (18)]. As a result, Eq. (20) holds approximately.

Second, we shall discuss the deviation from the half-Maxwellian in high temperature cases. To do so, we compare the velocity and temperature obtained from MD simulation and those evaluated using the kinetic theory on the assumption of the half-Maxwellian. In the kinetic theory, the velocity and temperature are given by

$$v_j=\frac{1}{\rho}\int \xi_j f d\boldsymbol{\xi},\quad T_j=\frac{1}{\rho R}\int(\xi_j-v_j)^2 f d\boldsymbol{\xi}. \tag{22}$$

The temperature is retrieved by $T=(T_x+T_y+T_z)/3$. Substituting the half-Maxwellian $f=2\rho_c\hat{f}^*=\alpha f^{\rm e}(\xi_z>0)$ into Eq. (22) gives

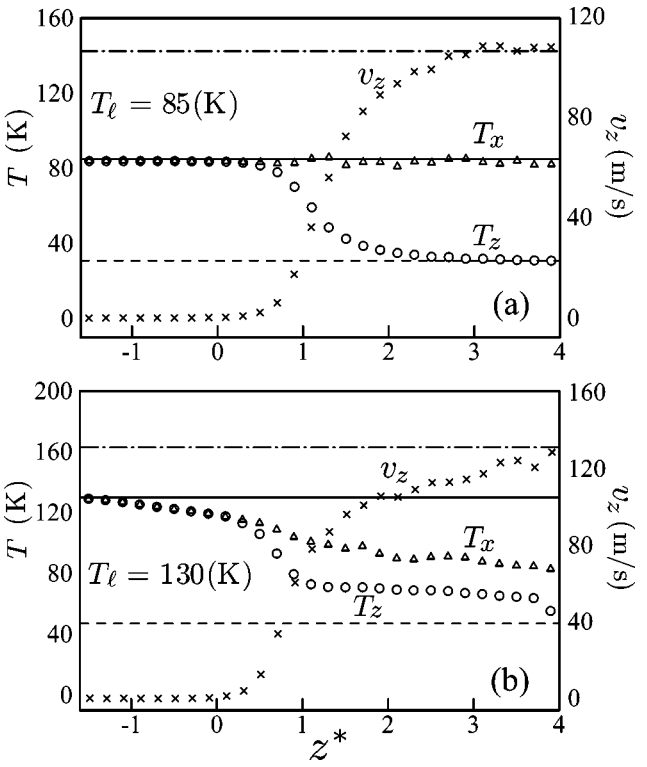

FIG. 10. Velocity and temperature of vapor evaporating into vacuum. (a) $T_\ell=85$ K, (b) $T_\ell=130$ K. Symbols are the results of vacuum simulations. The solid line represents $T_x=T_\ell$, the dash-dotted line v_z ($=106.1,130.3$ m/s), and broken line T_z ($=30.9,47.2$ K) given by Eqs. (23) and (24), respectively ($\Xi_p=L_xL_y\Delta z^*$, $\Delta z^*=0.2$).

$$v_x=v_y=0,\quad v_z=\sqrt{\frac{2RT_\ell}{\pi}}, \tag{23}$$

$$T_x=T_y=T_\ell,\quad T_z=\left(1-\frac{2}{\pi}\right)T_\ell. \tag{24}$$

Note that v_z and T_i's are independent of α. On the other hand, in MD simulations, the velocity and temperature can be calculated as

$$v_j=\frac{1}{\rho N_s\Xi_p}\sum_{N_s}\sum_{i\in\Xi_p} m^i\xi^i_j, \tag{25}$$

$$T_j=\frac{1}{\rho RN_s\Xi_p}\sum_{N_s}\sum_{i\in\Xi_p} m^i(\xi^i_j-v_j)^2, \tag{26}$$

where ξ^i_j is the j component of molecular velocity of the ith molecule. From Fig. 10(a), we can confirm that, at $z^*=4$ when $T_\ell=85$ K, the results from MD simulation agree with those by the kinetic theory on the assumption of the half-Maxwellian. In the case of $T_\ell=130$ K, however, the results from MD do not agree with those by the kinetic theory. In particular, the temperatures of tangential components to the interface T_x and T_y become definitely small compared with T_ℓ [see also Figs. 9(e) and 9(f)].

The most important factor that leads to the deviation form the half-Maxwellian in high temperature cases may be the molecular interaction in the transition layer. The useful measure for the molecular interaction is the Knudsen number for the transition layer Kn. A very rough estimation of Kn is $1/[\sqrt{2}\pi\sigma^2(\rho_v/m)\delta]$, where $\sigma=3.405$ Å [see Eq. (10)] and δ is the 10–90 thickness of the transition layer in the equilibrium state [see Eq. (12)]. Since Kn=43.1 for $T_\ell=85$ K, molecular collisions rarely happen in the transition layer in the low temperature case. Accordingly, the distribution function in the bulk condensed phase propagates toward the outside of the transition layer without deformation except for loosing the negative z^* component of molecular velocity. As a result, the vapor evaporates into the vacuum with the half-Maxwellian distribution. On the other hand, in the case of $T_\ell=130$ K, Kn=0.8 and therefore molecular collisions occur around $z^*=0$ [see Fig. 4(b)]. Since the intermolecular interaction promotes the local equilibration, $\hat{f}_x$ and $\hat{f}_z$ approach each other [see Figs. 9(e) and 9(e)].

V. CONCLUSIONS

Using the MD simulation of evaporation into vacuum, we have studied the physical appropriateness of the first term in the right-hand side of Eq. (1). First, we have demonstrated the existence of the spontaneous-evaporation flux $\langle J_{\mathrm{evap}}^{\mathrm{sp}}\rangle$ determined only by the temperature in the bulk condensed phase. The existence of $\langle J_{\mathrm{evap}}^{\mathrm{sp}}\rangle$ enables us to define $\langle J_{\mathrm{ref}}\rangle$ and $\langle J_{\mathrm{cnds}}\rangle$ by Eqs. (6) and (7), and hence the condensation coefficient α in equilibrium state is determined without any ambiguity. We have found that α is close to unity below the triple-point temperature and decreases as the temperature rises. Second, we have found that the distribution function of spontaneous evaporation $f_{\mathrm{evap}}^{\mathrm{sp}}$ is equal to the half-Maxwellian $\alpha f^{\mathrm{e}}(\xi_z>0)$ except for high temperature cases.

A number of analytical and numerical studies have so far been carried out in the area of molecular gas dynamics, where in addition to boundary condition, Eq. (1), the assumption of ideal gas also is important. By introducing $1-p_v/(\rho_v RT_\ell)$ as a measure of the deviation from the ideal gas, we have 0.03 for argon at 85 K and 0.28 at 130 K. The assumption of ideal gas may therefore be a good approximation for argon in low temperature cases treated here.

[1] C. Cercignani, *Rarefied Gas Dynamics* (Cambridge University Press, New York, 2000).

[2] Y. Sone, *Kinetic Theory and Fluid Dynamics* (Birkhäuser, Boston, 2002).

[3] The parameter α in the first term in Eq. (1) is sometimes called the evaporation coefficient and distinguished from the condensation coefficient. See Eq. (8), and also, R. Meland and T. Ytrehus, "Evaporation and condensation Knudsen layers for nonunity condensation coefficient," Phys. Fluids **15**, 1348 (2003).

[4] M. Matsumoto and Y. Kataoka, "Dynamic processes at a liquid surface of methanol," Phys. Rev. Lett. **69**, 3782 (1992).

[5] K. Yasuoka and M. Matsumoto, "Evaporation and condensation at a liquid surface. I. Argon," J. Chem. Phys. **101**, 7904 (1994).

[6] T. Tsuruta, H. Tanaka, and T. Masuoka, "Condensation/evaporation coefficient and velocity distributions at liquid–vapor interface," Int. J. Heat Mass Transfer **42**, 4107 (1999).

[7] G. Nagayama and T. Tsuruta, "A general expression for the condensation coefficient based on transition state theory and molecular dynamics simulation," J. Chem. Phys. **118**, 1392 (2003).

[8] R. Meland and T. Ytrehus, "Boundary condition at a gas–liquid interphase," in *Rarefied Gas Dynamics*, edited by T. J. Bartel and M. A. Gallis, AIP Conf. Proc. No. 585 (AIP, Melville, 2001), p. 583.

[9] R. Meland, "Molecular exchange and its influence on the condensation coefficient," J. Chem. Phys. **117**, 7254 (2002).

[10] A. Frezzotti and L. Gibelli, "A kinetic model for equilibrium and non-equilibrium structure of the vapor–liquid interface," in *Proceedings of the 23rd International Symposium on Rarefied Gas Dynamics*, edited by A. D. Ketsdever and E. P. Muntz, AIP Conf. Proc. No. 663 (AIP, New York, 2003), p. 980.

[11] M. Mecke, J. Winkelmann, and J. Fischer, "Molecular dynamics simulation of the liquid–vapor interface: The Lennard-Jones fluid," J. Chem. Phys. **107**, 9264 (1997).

[12] A. Trokhymchuk and J. Alejandre, "Computer simulations of liquid/vapor interface in Lennard-Jones fluids: Some questions and answers," J. Chem. Phys. **111**, 8510 (1999).

[13] J.-P. Hansen and L. Verlet, "Phase transitions of the Lennard-Jones system," Phys. Rev. **184**, 151 (1969).

[14] J. H. Dymond and B. J. Alder, "Pair potential for argon," J. Chem. Phys. **51**, 309 (1969).

[15] J. J. Burton, "Calculation of properties of solid argon from the Dymond–Alder potential," Chem. Phys. Lett. **15**, 312 (1970).

[16] Ch. Tegeler, R. Span, and W. Wagner, "A new equation of state for argon covering the fluid region for temperatures from the melting line to 700 K at pressures up to 1000 MPa," J. Phys. Chem. Ref. Data **28**, 779 (1999).

[17] W. H. Press, B. P. Flannery, S. A. Teukolsky, and W. T. Vetterling, *Numerical Recipes in C* (Cambridge University Press, Cambridge, 1988).

[18] M. P. Allen and D. J. Tildesley, *Computer Simulation of Liquids* (Clarendon, Oxford, 1987).

[19] S. I. Anisimov, D. O. Dunikov, S. P. Malyshenko, and V. V. Zhakhovskii, "Properties of a liquid–gas interface at high-rate evaporation," J. Chem. Phys. **110**, 8722 (1999).

[20] T. Tsuruta and G. Nagayama, "Molecular dynamics study on condensation coefficients of water," Trans. Jpn. Soc. Mech. Eng., Ser. A **68**, 1898 (2002) (in Japanese).

[21] M. Matsumoto, "Molecular dynamics of fluid phase change," Fluid Phase Equilib. **144**, 307 (1998).

[22] A. Thran, M. Kiene, V. Zaporojtchenko, and F. Faupel, "Condensation coefficients of Ag on polymers," Phys. Rev. Lett. **82**, 1903 (1999).

[23] K. J. Kossacki, W. J. Markiewicz, Y. Skorov, and N. I. Kömle, "Sublimation coefficient of water ice under simulated cometary-like conditions," Planet. Space Sci. **47**, 1521 (1999).

[24] S. Fujikawa, M. Kotani, H. Sato, and M. Matsumoto, "Molecular study of evaporation and condensation of an associating liquid," Heat Transfer-Jpn. Res. **23**, 595 (1994).

[25] H. K. Cammenga, "Evaporation mechanisms of liquids," Curr. Top. Mater. Sci. **5**, 335 (1980).

[26] The volume element in the vacuum simulation is fixed on the moving coordinate defined by Eq. (14).

[27] As a check of a necessary condition for statistical independence, we have confirmed that the correlation coefficients are small compared with unity.

[28] Exactly speaking, the condensed phase has a velocity$\approx\langle J_{\mathrm{evap}}^{\mathrm{sp}}\rangle/\rho_\ell$ in the moving coordinate. However, it is too small to be seen in Figs. 9(a) and 9(d).

[29] V. V. Zhakhovskii and S. I. Anisimov, "Molecular-dynamics simulation of evaporation of a liquid," JETP **84**, 734 (1997).